



## King's Research Portal

DOI:

[10.1016/j.ydbio.2019.03.017](https://doi.org/10.1016/j.ydbio.2019.03.017)

*Document Version*

Peer reviewed version

[Link to publication record in King's Research Portal](#)

*Citation for published version (APA):*

May, A. J., Teshima, T. HN., Noble, A., & Tucker, A. S. (2019). FGF10 is an essential regulator of tracheal submucosal gland morphogenesis. *Developmental Biology*, 451(2), 158-166.  
<https://doi.org/10.1016/j.ydbio.2019.03.017>

### **Citing this paper**

Please note that where the full-text provided on King's Research Portal is the Author Accepted Manuscript or Post-Print version this may differ from the final Published version. If citing, it is advised that you check and use the publisher's definitive version for pagination, volume/issue, and date of publication details. And where the final published version is provided on the Research Portal, if citing you are again advised to check the publisher's website for any subsequent corrections.

### **General rights**

Copyright and moral rights for the publications made accessible in the Research Portal are retained by the authors and/or other copyright owners and it is a condition of accessing publications that users recognize and abide by the legal requirements associated with these rights.

- Users may download and print one copy of any publication from the Research Portal for the purpose of private study or research.
- You may not further distribute the material or use it for any profit-making activity or commercial gain
- You may freely distribute the URL identifying the publication in the Research Portal

### **Take down policy**

If you believe that this document breaches copyright please contact [librarypure@kcl.ac.uk](mailto:librarypure@kcl.ac.uk) providing details, and we will remove access to the work immediately and investigate your claim.

1  
2  
3 FGF10 is an essential regulator of tracheal submucosal gland  
4  
5 morphogenesis  
6  
7  
8  
9  
10

11  
12 Alison J. May<sup>1</sup>φ, Tathiane H.N. Teshima<sup>1,2</sup>, Alistair Noble<sup>3</sup> and Abigail S. Tucker<sup>1</sup>§  
13  
14

15  
16 <sup>1</sup>Centre for Craniofacial and Regenerative Biology, Guy's Hospital, King's College London,  
17 United Kingdom  
18

19 <sup>2</sup>Department of Stomatology, School of Dentistry, University of Sao Paulo, Brazil  
20

21 <sup>3</sup>MRC & Asthma UK Centre in Allergic Mechanisms of Asthma, King's College London, United  
22 Kingdom  
23  
24

25  
26 § author for Correspondence

27 [abigail.tucker@kcl.ac.uk](mailto:abigail.tucker@kcl.ac.uk)  
28  
29

30  
31 φ Current address: Program in Craniofacial Biology, Department of Cell and Tissue Biology,  
32 University of California, 513 Parnassus Avenue, San Francisco, CA, 94143, USA.  
33  
34  
35  
36  
37  
38  
39  
40  
41  
42  
43  
44  
45  
46  
47  
48  
49  
50  
51  
52  
53  
54  
55  
56

## Abstract

Mucus secretion and mucociliary clearance are crucial processes required to maintain pulmonary homeostasis. In the trachea and nasal passages, mucus is secreted by submucosal glands (SMGs) that line the airway, with an additional contribution from goblet cells of the surface airway epithelium. The SMG mucus is rich in mucins and antimicrobial enzymes. Defective tracheal SMGs contribute to hyper-secretory respiratory diseases, such as cystic fibrosis, asthma, and chronic obstructive pulmonary disease, however little is known about the signals that regulate their morphogenesis and patterning. Here, we show that *Fgf10* is essential for the normal development of murine tracheal SMGs, with gland development arresting at the early bud stage in the absence of FGF10 signalling. As *Fgf10* knockout mice are lethal at birth, inducible knockdown of *Fgf10* at late embryonic stages was used to follow postnatal gland formation, confirming the essential role of FGF10 in SMG development. In heterozygous *Fgf10* mice the tracheal glands formed but with altered morphology and restricted distribution. The reduction in SMG branching in *Fgf10* heterozygous mice was not rescued with time and resulted in a reduction in overall tracheal mucus secretion. *Fgf10* is therefore a key signal in SMG development, influencing both the number of glands and extent of branching morphogenesis, and is likely, therefore, to play a role in aspects of SMG-dependent respiratory health.

**Keywords:** Branching morphogenesis, development, airway, fibroblast growth factor, respiratory disease

## Introduction

Airway mucus secretion plays a critical role in the muco-ciliary clearance of billions of airborne particles and pathogens daily. Respiratory mucus is produced by the goblet cells of the surface epithelium and the submucosal glands (SMGs) found within the submucosal layer of the nasal, tracheal and bronchial cavities (Sturgess & Imrie 1982; Borthwick et al. 1999; May & Tucker 2015). The structure of tracheobronchial SMGs are characterized into three domains: (1) the distal secretory gland, (2) the medial collecting duct and (3) the proximal ciliated duct (*reviewed in* May & Tucker 2015). The distal region consists of two distinct secretory cell types, responsible for producing airway mucus. Serous cells produce a solution primarily consisting of mucin MUC7, proteoglycans and bactericidal proteins such as lactoferrin and lysozyme (Masson et al. 1966; Klockars & Reitamo 1975; Finkbeiner 1999) while mucous cells produce a gel rich in MUC2 and MUC5b and antimicrobial peptide cathelicidin (Buisine et al. 1999; Finkbeiner 1999). Collectively these secretions provide a barrier to the exposed surface airway epithelium. While the cellular composition of SMGs is homologous across mammals, SMG distribution can change between species. In mice, respiratory SMGs are found within the walls of the nasal cavity and extend to the upper trachea, with most tracheal SMGs found between the cricoid cartilage and the first tracheal cartilage ring. SMGs in mice only extend to the seventh cartilage ring, however in humans glands extend more caudally throughout the trachea and bronchi (Borthwick et al. 1999; Sturgess & Imrie 1982).

The need to understand the morphogenesis, structure and function of the SMGs is emphasised by the role they play in respiratory diseases such as cystic fibrosis (CF), asthma and chronic obstructive pulmonary disease (COPD). Decreased mucus secretion from tracheal and nasal SMGs is characteristic of humans with CF (Joo et al. 2010; Salinas et al. 2005; Jeong et al. 2015), contributing to decreased mucociliary clearance of the airways and onset of pulmonary infection. Further evidence in the pig model of CF shows that mucus hypo-secretion (Joo et al. 2010; Cho et al. 2011), and increased mucus tethering from the SMGs (Hoegger et al. 2014) give rise to hindered muco-ciliary clearance, prior to the onset of inflammation, indicative that SMG morphology and function are primary defects of CF pathogenesis. Mouse models of CF have shown to have abnormal distribution of tracheal SMGs, with an increase in proximal numbers of SMGs in diseased animals (Borthwick et al. 1999). Moreover, early onset of hypertrophy in SMGs is

characteristic of infants with CF (Oppenheimer & Esterly 1975; Sturgess & Imrie 1982). Chronic asthma sufferers also show signs of SMG secretory cell hyperplasia (Aikawa et al. 1992; Rogers 2004), while sufferers of COPD show mucous cell hyperplasia that gives rise to mucus-hypersecretion and airway plugging (Reid 1960; Rogers 2008).

Development of SMGs undergoes typical patterns common to other branching organs such as the lung, salivary gland and mammary gland (Tucker 2007; Hannezo et al. 2017). Tracheal SMG morphogenesis can be described in four stages (Keswani et al. 2011; Thurlbeck et al. 1961). Stage 1 of development defines the specification and emergence of an initial gland bud from the respiratory epithelium (Figure 1, A). Stage 2 is characterised by elongation of the epithelial bud into the underlying mesenchyme, and the onset of cavitation within the stalk as lumen formation begins (Figure 1, A). Stage 3 describes the continual clefting and branching of the SMG, alongside lumen formation. Stage 4 is classified by cellular differentiation, indicated by mucus production within the distal glandular secretory cells (Figure 1, A).

A few studies have shed light on the signalling pathways involved in tracheal SMG development and patterning. *Eda/Edaradd* expression is required for early gland initiation and budding as tracheal SMG number is severely reduced in both the *Tabby* (*Eda* mutant), and *Crinkled* mouse (*Edaradd* mutant) at postnatal day 7 (Rawlins & Hogan 2005). Furthermore, human patients with hypohidrotic ectodermal dysplasia, caused by defects in the EDA pathway, have reduced numbers of respiratory SMGs, asthma-like symptoms, and respiratory tract infections (Callea et al. 2013). *Wnt/β-catenin* activation of lymphoid enhancer factor *Lef-1* is also required for early SMG bud specification and outgrowth (Xie et al. 2014). The transcription factor Sox2 inhibits expression of the *Lef-1*, while WNT signalling reduces Sox2 expression in the SMG placode. Therefore, WNT signalling leads to reduced SOX2 and an increase of *Lef-1* transcripts in SMG placodes, suggesting a dynamic relationship between WNT signalling and Sox2 expression during SMG bud specification (Xie et al. 2014).

In vertebrates, fibroblast growth factors (FGFs) make up one of the largest family of polypeptide proteins with 22 ligands (FGF1-FGF22) and four cell membrane-bound FGF receptors (FGFRs)(Ornitz & Itoh 2001). FGF10/FGFR2b signalling is required for successful development

of many branched organs (Ohuchi et al. 2003). Lung morphogenesis is inhibited in the absence of *Fgf10* and *Fgfr2b* expression, and *Fgf10* and *Fgfr2b* homozygous mice die at birth due to lung agenesis (Sekine et al. 1999; Min et al. 1998; De Moerlooze et al. 2000). Morphogenesis of the submandibular salivary gland is arrested at the initial bud stage at embryonic day E12.5 in both *Fgf10* and *Fgfr2b* homozygous (-/-) mice, and salivary glands are hypoplastic and secrete a reduced volume of saliva in *Fgf10* heterozygous (+/-) adults (May et al. 2015). More recently it has been shown that *Fgf10* maintains *Sox9* expression and regulates SOX9+ epithelial progenitor cell expansion during salivary gland morphogenesis (Chatzeli et al. 2017).

The tracheal SMGs have not been investigated in the complete absence of FGF10 signalling, however *Fgf10* heterozygous mice have a reduction in the number of SMGs at postnatal day 20 compared to wildtype littermates (Rawlins & Hogan 2005). The glands present in the tracheal submucosa had undergone less branching and were restricted to the anterior trachea, with no glands found between the more posterior cartilaginous rings (Rawlins & Hogan 2005). Considering this altered phenotype, we investigated the role of FGF10 in early tracheal SMG development using both knockout and conditional knockout mice.

## Materials and Methods

### Experimental Animals

*Fgf10*-deficient mice were first generated by Min et al. (1998) (Mouse Genome Informatics ID 1099809). Investigation was carried out on WT (n=3), *Fgf10* +/- (n=2) and *Fgf10* -/- (n=4) for P0 SMG analysis and WT (n=7) and *Fgf10* +/- (n=6) for adult SMG analysis. For inducible ablation experiments, the ubiquitous *pCAGGCre-ERT2* allele (Hayashi and McMahon, 2002) was crossed to *Fgf10* floxed (*Fgf10A02 tmc1c*) mice on a C57BL/6 background (produced by MRC-Harwell as part of the International Mouse Phenotyping Consortium (IMPC; Skarnes et al. 2011; Bradley et al. 2012). *Fgf10*<sup>fl/fl</sup> females were crossed to *pCAGCre-ERT2*+/+;*Fgf10*<sup>fl/+</sup> males to generate wildtype *pCAGCre-ERT2*+/+;*Fgf10*<sup>fl/fl</sup> (WT;*Fgf10*<sup>fl/fl</sup>, n=3), *pCAGCr-eERT2*+/+;*Fgf10*<sup>fl/+</sup> (*Cre*<sup>ERT2</sup>;*Fgf10*<sup>fl/+</sup>, n=3) and *pCAGCre-ERT2*+/+;*Fgf10*<sup>fl/fl</sup> (*Cre*<sup>ERT2</sup>;*Fgf10*<sup>fl/fl</sup>, n=3) mouse pups which were collected at postnatal day (P)21. *R26-tdTomato* reporter line (Gt(ROSA)26 Sor tm14(CAG-tdTomato)Hze JAX labs) was used to confirm the activity of the *Cre* induced by tamoxifen and were mated to *Fgf10*<sup>fl/fl</sup> males to generate *Fgf10*<sup>fl/fl</sup>;*R26RtdTom* females. These

281  
282  
283 were mated to *PCAGcreERT2/+;Fgf10<sup>fl</sup>/+* males and the Tomato was observed with a Nikon  
284 SMZ25 fluorescence microscope. *Fgf10/lacZ/+* reporter mice carrying a nuclear-targeted lacZ  
285 insertion that does not disrupt *Fgf10*'s coding exons, were mated and postnatal pups were provided  
286 by Mohammad Hajihosseini (n = 3) (Kelly et al., 2001; Hajihosseini et al., 2008). All procedures  
287 and culling methods were performed under a project license approved by the United Kingdom's  
288 Home Office and in accordance with the Animal (Scientific Procedures) Act of 1986, United  
289 Kingdom.  
290  
291  
292  
293  
294

### 295 ***Animal Collection***

296 Mice were mated in the late evening and a midnight mating was assumed. Midday of the day at  
297 which a vaginal plug was discovered was recorded as embryonic day (E) 0.5. Adult males and  
298 females were culled by exposure to rising levels of CO<sub>2</sub> gas. Primers used to detect wildtype *Fgf10*  
299 locus were 5'-GAGGAAATGCTGCGCACAATGTATACTCGG-3' (Fgf203 forward primer)  
300 and 5'-GGATACTGACACATTGTGCCTCAGCCTTTC-3' (Fgf204 reverse primer) while the  
301 mutant *Fgf10* locus was detected by primers 5'-GCTTGGGTGGAGAGGCTATTC-3' (Fgf233  
302 forward primer) and 5'-CAAGGTGAGATGACAGGAGATC-3' (Fgf234 reverse primer) of the  
303 neo-cassette insert (Sekine et al. 1999). The inducible loss of *Fgf10* was performed by  
304 administering 75mg of tamoxifen/kg body weight intraperitoneally in corn oil into E17.5 pregnant  
305 mice, and 15µg/g into each pup at postnatal day 2. Corn oil injections alone has been shown to  
306 lead to no activation of this *Cre* line (Hayashi & McMahon, 2002). E17.5 was chosen as this is 24  
307 hours prior to the induction of SMG in the trachea (May & Tucker, 2015). Tamoxifen  
308 recombination time was expected to occur 24h after administration (Danielian et al., 1998).  
309 Tamoxifen was injected in combination with progesterone to counter the negative effects of  
310 tamoxifen on the ability to give birth naturally (Lizen et al., 2015). At this dose of tamoxifen the  
311 recombination of this *Cre* line is not 100% penetrant (Hayashi & McMahon, 2002). Therefore a  
312 second injection was given postnatally at P2. Mice were then culled at postnatal day 21.  
313  
314  
315  
316  
317  
318  
319  
320  
321  
322  
323  
324

### 325 ***Histological Staining***

326 Upon collection, trachea were fixed in 4% paraformaldehyde in PBS (PFA) overnight at 4°C.  
327 Tissue was dehydrated in increasing methanol concentrations and left overnight at 4°C in  
328 Isopropanol (Sigma Aldrich). Samples were cleared in 1,2,3,4 Tetrahydronaphthalene at RT, and  
329  
330  
331  
332  
333  
334  
335  
336

337  
338  
339 embedded in paraffin wax. Alternative serial 9µm sagittal sections were collected along  
340 dorsal/ventral axis of each trachea. Paraffin embedded sections were dewaxed using Histoclear  
341 and rehydrated through an ethanol series. Tracheal sections were stained using a Trichrome stain  
342 of 1% Alcian Blue, Ehrlich's Haematoxylin and 0.5% Sirius Red in saturated Picric Acid.  
343  
344  
345

#### 346 347 348 ***X-gal staining of *Fgf10* LacZ<sup>±</sup> postnatal submucosal glands***

349 Trachea of postnatal day 7 (P7) were fixed in PFA 4% overnight at 4°C, followed by two washes  
350 in 2µM of magnesium chloride (MgCl<sub>2</sub>) in PBS for 5 and 15 minutes at RT. Samples were then  
351 washed in a solution of 0.1% of Deoxycholic Acid, 0.2% of Igepal NP-40, 1µM of MgCl<sub>2</sub> in PBS  
352 for 5 minutes at RT. Staining was performed using previous solution with 5mM of K<sub>3</sub>Fe(CN)<sub>6</sub>,  
353 5mM of K<sub>4</sub>Fe(CN)<sub>6</sub> and 1mg/mL of X-gal in Dimethyl sulfoxide (DMSO) overnight at 37°C.  
354 Samples were washed in PBS and post-fixed in PFA overnight at 4°C to stop reaction, followed  
355 by paraffin embedding process. Sections of 15µm were then counterstained in 0.5% of alcoholic  
356 eosin and mounted with Neomount (Merck Millipore).  
357  
358  
359  
360  
361  
362

#### 363 364 ***Cartilaginous staining of embryonic tracheal tissue***

365 Trachea were dissected from E18.5 *Fgf10* WT and *Fgf10* <sup>±</sup> littermates and fixed overnight in  
366 95% ethanol in deionised H<sub>2</sub>O at 4°C. After 24 hours of fixation, fat from tissue was removed by  
367 storing trachea in 100% acetone overnight at RT. Followed by two rinses in 95% ethanol, trachea  
368 were placed in Alcian Blue solution (15mg Alcian Blue 8GX in 80ml 95% ethanol and 20ml glacial  
369 acetic acid) for 24 hours rocking at RT. Tissue was rinsed with 95% ethanol twice for 30 minutes  
370 and stored in 95% ethanol overnight at RT. Trachea were cleared in 1% Potassium Hydroxide  
371 (KOH) for 3-4 hours. Tissue went through a series of 1% KOH and glycerol solutions, at RT.  
372 Tissue was stored in 100% glycerol imaged using a Leica MZFLiii dissection microscope fixed  
373 with a Leica DFC300 Fx camera.  
374  
375  
376  
377  
378  
379  
380

#### 381 382 ***Mucus secretion analysis***

383 Mice aged 7-8 weeks (WT; n=4, *Fgf10* <sup>±</sup>; n=6) were culled by exposure to rising levels of CO<sub>2</sub>  
384 and trachea were immediately dissected. The thyroid gland and oesophagus were removed, and  
385 the trachea was cut along the dorsal trachealis muscle (Supplementary Figure 1, A). The following  
386  
387  
388  
389  
390  
391  
392



procedure was modified from the method used (Ianowski et al. 2007). Using insect pins, the trachea was opened and pinned to a sylgard plate and the luminal mucosal surface was exposed (Supplementary Figure 1, B). The mucosal side of each trachea was dried with air spray and 5µl of mineral oil (Sigma) was added to the surface. Beneath the trachea, 2.5µl of D-MEM/F12 plus penicillin/streptomycin and 1% Glutamax (Invitrogen) medium was added to nourish the tissue during incubation (Supplementary Figure 1, B). Tracheal tissue placed in a 95% O<sub>2</sub>: 5% CO<sub>2</sub> incubator at 37°C for 10 minutes. The exposed trachea was placed under a Leica MZFLi dissection microscope fitted with a Leica DFC300 Fx digital camera. A further 2.5µl of DMEM/F12 medium containing 60µM of the cholinergic carbachol (Sigma) was added to the medium bath, giving a final concentration of 30µM carbachol stimulating the tracheal glands. Photographs of the anterior region of the trachea were taken every 30 seconds for 10 minutes to trace mucus bubble production.

After 10 minutes of exposure to carbachol, the total number of mucus bubbles produced were counted. Viable bubbles for area measurement were those of which followed the criteria described in Ianowski et al. (2007): (a) a complete circular outline surrounding each mucus bubble as accurate measurements could be collected and (b) no fusion with adjacent droplets. For gland opening analysis these criteria were not followed, as they were not required to count the amount of bubbles produced. Area of each bubble was calculated in micrometres (µm<sup>2</sup>) ImageJ software. Overall trachea mucus secretion was calculated by the sum of all areas of each bubble per animal. Statistics and graphs were calculated using Microsoft Excel and Graphpad Prism software.

## Results

### ***Complete loss of Fgf10 leads to defective tracheal SMG development***

To investigate the role of *Fgf10* during early stages of tracheal SMG development, glands were analysed in *Fgf10* +/- and *Fgf10* -/- mice. Although *Fgf10* -/- mice die at birth due to lung agenesis (Min et al. 1998; Sekine et al. 1999), initiation of SMGs can be analysed as anterior glands start to emerge from the tracheal epithelium at Embryonic day (E)18.5 (May & Tucker 2015). *Fgf10* mutant pups were collected on E19/P (postnatal day) 0 as the mother was giving birth. In wildtype (WT) animals, glands had budded, elongated, cavitated and commenced branching (Figure 1, B, B'). Similar stages of development were seen in heterozygous (*Fgf10* +/-) littermates however

gland development appeared delayed and branching of the formed glands reduced (Figure 1, C, C'). In the complete absence of *Fgf10* in homozygous animals (*Fgf10*<sup>-/-</sup>), some gland buds were found emerging from the surface epithelium, however development was arrested at this bud initiation stage, with no glands found at a distance from the tracheal surface (Figure 1, D, D'). This indicates that the SMGs did not undergo later stages of branching morphogenesis and that *Fgf10* expression is not required for initial epithelial gland bud specification but is required for subsequent successful bud elongation and branching.

### ***Time inducible loss of Fgf10 during postnatal development reduces anterior tracheal SMG branching and posterior SMG expansion***

To further investigate the role of *Fgf10* during SMG morphogenesis, we turned to later stages of postnatal gland development. First, we analysed *Fgf10* expression in *Fgf10*<sup>LacZ/+</sup> mice at P7. Xgal staining revealed *Fgf10* expression in the mesenchyme surrounding the developing SMG (Figure 2, A). To follow development of the tracheal SMGs at postnatal stages we moved to a time inducible *Fgf10* knockout mice (*Cre*<sup>ERT2</sup>;*Fgf10*<sup>fl/fl</sup>;*tdTom*). Tamoxifen was administered to pregnant females at E17.5, just as the most anterior tracheal SMGs were starting to initiate, and again to individual pups at P2, with tracheal tissue collected at P21 (Figure 2, B). As *Fgf10*<sup>-/-</sup> mice die at birth, due to agenesis of the lungs (Sekine et al. 1999; Min et al. 1998), ablation of FGF10 using the inducible knockout mouse allowed pups to develop to E17.5 with adequate FGF10 expression, but permitted our continued study of SMG development in the absence of FGF10 from E18.5. Earlier injection was not attempted due to potential compromised development of the palate, which is reliant on *Fgf10* expression (Rice et al. 2004; Teshima et al. 2016). Tamoxifen inducible *Cre* recombination was confirmed in the anterior and posterior trachea by the expression of R26tdTomato (red – Figure 2, C). No Tomato was observed in control *Cre* negative *Fgf10*<sup>fl/fl</sup>;*tdTom* pups (Figure 2, C). Trichrome staining of tracheal sections concluded a significant loss of anterior SMG branching adjacent to the cricoid cartilage in *Cre*<sup>ERT2</sup>;*Fgf10*<sup>fl/fl</sup> animals compared to control *Cre* negative littermates (Figure 2 D, orange outline). A slight reduction in anterior SMG branching was observed in heterozygous *Cre*<sup>ERT2</sup>;*Fgf10*<sup>fl/+</sup> littermates (Figure 2, D). Additionally, an absence of SMGs located posterior to the cricoid cartilage, in between the tracheal cartilage rings was evident in both *Cre*<sup>ERT2</sup>;*Fgf10*<sup>fl/+</sup> and *Cre*<sup>ERT2</sup>;*Fgf10*<sup>fl/fl</sup> animals, while in control

mice SMGs reached the 4th cartilage ring (C4)(Figure 2 D-E). These results further support the necessity of *Fgf10* in tracheal SMG elongation and branching.

#### ***Anterior and posterior tracheal SMGs are reduced in *Fgf10*<sup>+/-</sup> adult mice***

It has previously been reported that there is an altered SMG phenotype in adult *Fgf10*<sup>+/-</sup> mice, with a reduction in branching of the anterior SMGs adjacent to the cricoid cartilage and a severe reduction in the posterior expansion of the glands between each tracheal cartilage ring in adult *Fgf10*<sup>+/-</sup> (Rawlins & Hogan 2005). We investigated adult WT and *Fgf10*<sup>+/-</sup> littermates and observed a similar phenotype in our mouse line with a reduction in anterior tracheal SMGs in heterozygous animals compared to their WT littermates (Figure 3, A). Variation in severity of this reduction was observed in *Fgf10*<sup>+/-</sup> mice however the number of glands was always decreased in the heterozygous adults compared to WT littermates (Figure 3, A and B). Analysis of SMGs between tracheal cartilage rings also showed a notable reduction in the anterior-posterior presence of the glands (Figure 3, B). The majority of WT littermates showed continuous SMG development between each cartilage ring, most often reaching the mesenchyme between the 6<sup>th</sup> and 7<sup>th</sup> ring (Figure 3, B). In *Fgf10*<sup>+/-</sup> mice, posterior expansion of the SMGs was significantly reduced, with small SMGs only found above the 3<sup>rd</sup> cartilage ring. In a previous study investigating tracheal SMG formation in the *Tabby* mouse, which has deficient *Eda* signalling, the pseudostratified epithelium of the trachea showed a disorganized appearance and increased height of columnar epithelial cells compared to WT animals (Rawlins & Hogan 2005). In our study, no epithelial abnormalities were observed in the *Fgf10*<sup>+/-</sup> animals compared to their WT littermates (Figure 3, C).

*Fgf10* has been shown to be expressed in the ventral tracheal mesenchyme from E12.5-E16.5 when tracheal patterning is underway (Sala et al. 2011). Additionally, *Fgf10* null embryos have truncated trachea with disorganized rings (Sala et al. 2011). As SMGs form between the tracheal cartilage rings, we wanted to ensure that the observed altered SMG phenotype in *Fgf10*<sup>+/-</sup> animals was not a secondary defect to abnormal cartilage patterning. This hypothesis was ruled out using whole mount Alcian Blue staining, however, as no difference in cartilage phenotype between WT and *Fgf10*<sup>+/-</sup> littermates was observed (Supplementary Figure 1, A).

#### ****Fgf10*<sup>+/-</sup> adult mice showed reduced tracheal SMG openings and overall mucus secretion***

Using histological methods, it was difficult to conclude whether the heterozygous mice showed a reduction in branching of each gland, a reduction in the number of glands within the anterior mesenchyme, or collectively both of these mechanisms. We therefore moved to a live tracheal explant model to follow mucous production. Previous papers have used the application of mineral oil to the mucosal tracheal surface to investigate SMG fluid secretion (Joo et al. 2001; Ianowski et al. 2007). We therefore used this model to assess whether the defect in branching led to a reduction in the amount of mucus secreted into the airway lumen in heterozygous animals compared to their WT littermates (Supplementary Figure 1, B and C). A time line of images was taken of the tracheal tissue in culture during mucus production stimulated by carbachol over a 10-minute period. Images were analysed and the number of mucus bubbles present between the cricoid cartilage (CC) and Tracheal cartilage 2 (C2) were counted. Each bubble represented the presence of a gland opening. Results elucidated that the amount of bubbles was significantly reduced in *Fgf10* +/- animals ( $p<0.001$ ), indicating a decrease in the number of functional glands within the mesenchyme of the trachea between the anterior cartilage rings in *Fgf10* +/- adults (Figure 4, A and B). While analysis of the area of each individual bubble did not differ significantly between the two groups ( $p=0.429$ ), the overall amount of mucus secreted (sum of all bubble areas) was significantly reduced in *Fgf10* +/- adults (Figure 4, B,  $p<0.001$ ). Together with the histological analysis of *Fgf10* heterozygous adult mice, these results indicate a reduction in total mucus secreted within the tracheal lumen compared to WT littermates, which is due to a combination of both reduced gland number and reduced gland branching.

## Discussion

The present study takes a number of approaches to show that Fgf10 signalling is essential for the development of tracheal submucosal glands. Our results conclude that although SMG bud initiation and outgrowth may be Fgf10 independent, the later stages of gland branching, cellular differentiation and gland secretion are significantly compromised in the absence of *Fgf10* expression.

As anterior tracheal SMGs in the ventral part of the tube start initiating at E18.5 in our mouse line, this gave us an opportunity to collect *Fgf10* -/- pups at P0, along with their WT and *Fgf10* +/- littermates, to investigate the effect of loss of Fgf10 on gland initiation. Interestingly, gland buds

were found in the ventral and slightly more dorsal anterior positions in the *Fgf10* <sup>-/-</sup> specimens collected. This result showed that *Fgf10* is not required for the initiation of the epithelial gland primordia or the outgrowth of the initial gland bud, however it is essential for glands to progress to later development. The role of FGF10 in these later morphogenetic stages was further supported by a reduction in SMG branching observed in *Fgf10* <sup>+/-</sup> pups at P0. Ventral glands of WT animals had reached the lumen formation stage and were undergoing clefting and branching while *Fgf10* <sup>+/-</sup> littermates displayed glands that had elongated into the underlying mesenchyme and formed lumens but showed evident reduced branching. This phenotype mirrors that reported for both the submandibular salivary gland (Jaskoll et al. 2005; Wells et al. 2013; Teshima et al. 2016; Chatzeli et al. 2017) and mammary gland (Mailleux et al. 2002) in *Fgf10* <sup>-/-</sup> mice, where gland development does not progress passed the bud stage and branching is reduced leading to aplastic glands. This suggests that FGF10 signalling in particular is not needed for initial gland outgrowth, a conserved role reported in a variety of glandular organs, but is essential for subsequent development stages and that other ligands are essential for initial gland budding. One such factor may be FGF7, which also signals through FGFR2b. *Ex vivo* studies of the developing submandibular salivary gland have shown that FGF7, through activated MEK and PI3K signalling cascades, is required for salivary gland budding, and that FGF10 promotes branching and elongation of gland ducts through MEK 1/2 signalling (Steinberg et al., 2005). Furthermore, both recombinant human FGF7 and FGF10 induce ectopic bud formation of the lacrimal gland epithelium in mouse embryonic ocular cultures (Makerenkova et al., 2000). This suggests that FGF7 may promote SMG initial bud formation, or even compensation in the absence of FGF10 signalling to induce SMG bud outgrowth. Furthermore, we previously showed that *Fgf10* expression is essential for a subset of nasal glands, with other *Fgfs* compensating for the loss of *Fgf10* in some glands (May et al. 2016). The lateral nasal glands, for example, only require *Fgf10* for later gland branching stages, while the Steno's gland and the sinus glands require *Fgf10* expression earlier at gland initiation stages (May et al. 2016). The SMGs therefore show a reliance on FGF10 signalling more similar to the stenoses and sinus glands.

As previously reported in other glands (May et al. 2016; Chatzeli et al. 2017), here we show that *Fgf10* is expressed in the tracheal mesenchyme adjacent to the gland epithelium during branching morphogenesis at P7. Due to agenesis of the lungs, *Fgf10* <sup>-/-</sup> mice die at birth (Sekine et al. 1999;

Min et al. 1998), thereby preventing the study of later stages of tracheal gland development in the null mutant. Therefore, we adopted the use of a conditional *Fgf10* ablation model to investigate if tracheal SMGs could develop postnatally in the absence of FGF10 signalling. Ablation of *Fgf10* was induced at E17.5 and P2 and tracheal tissue was collected at P21. Histological analysis revealed a significant reduction in branching of the anterior glands adjacent to the cricoid cartilage in *CreERT2;Fgf10<sup>fl/fl</sup>* mice compared to wildtype littermates. Although minimal, some branching and cellular differentiation (indicated by mucus staining - blue) had occurred in the anterior gland epithelia. As our first tamoxifen administration may have taken 24 hours to induce Cre-recombination, some residual FGF10 may have promoted branching and mucus production in few SMG primordia that had initiated by E17.5/E18.5. Furthermore, as 100% Cre-recombination cannot be guaranteed, again some SMG placodes may have been exposed to low levels of FGF10, inducing some cellular differentiation. To this end, mucus cell differentiation was indicated by alcian blue staining alone and to conclude the role of FGF10 in cellular differentiation, analysis of differentiation markers such as AQP5 (Song et al., 2001) and MUC5b (Roy et al., 2014) is required. In contrast, posterior SMGs that develop postnatally were reduced in *CreERT2;Fgf10<sup>fl/+</sup>* mice and completely absent in *CreERT2;Fgf10<sup>fl/fl</sup>* mice at P21, while found to extend to C4 in WT littermates. This phenotype suggests one of two strategies: (1) bud outgrowth had occurred, however loss of *Fgf10* caused cell death in gland epithelium leading to no SMG buds evident by P21; or (2) FGF10 is required for gland initiation and bud outgrowth in more posterior SMGs. In support of the latter, heterogeneous progenitor cell populations and signalling mechanisms are known to occur in the lung epithelium in an anterior/posterior axis. Cytokeratin-5 positive basal cells replenish the airway epithelium in the anterior trachea (Rock et al. 2009), while Clara cells are understood to be the main stem cell population of the more posterior tracheal epithelium (Rawlins et al. 2009). More recently, a study investigating airway epithelial regeneration following severe injury showed a multipotent SMG myoepithelial progenitor replenished airway epithelium in the anterior trachea (between CC-C1), with reduced replenishment observed in the posterior epithelium (C1-C4)(Lynch et al. 2018). Considering these heterogeneous mechanisms, while FGF10 may not be essential for anterior SMG bud initiation, it may be required for bud outgrowth in more posterior glands. This may also explain the phenotype observed in adult *Fgf10* +/- mice, where the posterior glands are more strongly affected. It is understood that mesenchymal FGF10 regulates progenitor cell proliferation in adjacent branching epithelial structures in a number of

different organs, such as the lung (Ramasamy et al. 2007), pancreas (Bhushan et al. 2001) and salivary gland (Chatzeli et al. 2017). For example, analysis of PCNA positive cells during lung development with reduced FGF10 signalling revealed a significant decrease in proliferating cells in the lung epithelium, while proliferation was unchanged in the mesenchyme population (Ramasamy et al. 2007). Further analysis of cell proliferation in both the anterior and posterior trachea will give insight into the role of FGF10 in regulating this process in tracheal SMGs. Furthermore, the altered SMG phenotype in the conditionally ablated *Fgf10* model, and the global *Fgf10* heterozygous mouse is similar to the aplastic lacrimal and salivary gland phenotypes observed in patients that suffer from both ALSG and LADD syndrome (Milunsky et al. 2006; Shams et al. 2007; Entesarian et al. 2007). While no reports have stated any pulmonary defects in patients with ALSG or LADD syndrome, the airway SMGs may show aplasia and this phenotype could possibly give rise to muco-ciliary deficiencies in those that suffer from these autosomal dominant diseases. Furthermore, our functional tests of mucus secretion in *Fgf10* +/- adult mice conclude a significant reduction in total amount of mucus secreted into the airway lumen. As only the anterior glands were included in the study, an even greater difference would be assumed if all mucus bubbles extending posteriorly in WT animals had been calculated.

In addition, previous reports have indicated SMG development has ended by P21 in the mouse trachea (Rawlins and Hogan, 2005). However, in our analysis, WT mice only had SMGs extending down to the 4<sup>th</sup> tracheal cartilage ring (C4) at P21, in comparison to the 6-8 week WT mice where glands were observed at much more posterior levels (Figure 3, B). We therefore believe that posterior initiation of glands still occurs after 3 weeks. To this end, we report that tracheal mesenchymal *Fgf10* expression is essential for tracheal submucosal gland morphogenesis, in both late embryonic and early postnatal stages. Without this signalling factor, glands fail to develop, arresting at the bud stage anteriorly. Investigation into this developmental signalling cascade should be considered in further research attempting to understand the role of these organs in hyper-secretory respiratory diseases.

## Acknowledgements

We would like to thank the Dental Institute of King's College London (Tucker, 2011) for funding May AJ. Teshima THN was funded by FAPESP (Fundação de Amparo à Pesquisa do Estado de

São Paulo) (grant 2015/02824). Thanks to Mohammad Hajihosseini (University East Anglia) for the Fgf10LacZ reporter mice. The Fgf10A02 tmc1c mice were obtained from the MRC-Harwell, which distributes these mice on behalf of the European Mouse Mutant Archive (<http://www.emmanet.org>). The MRC-Harwell is also a member of the International Mouse Phenotyping Consortium (IMPC), which funded the generation of the Fgf10A02 tmc1c mice. Associated primary phenotypic information may be found at <http://www.mousephenotype.org>.

## References

- Aikawa, T. et al., 1992. Marked goblet cell hyperplasia with mucus accumulation in the airways of patients who died of severe acute asthma attack. *Chest*, 101(4), pp.916–21.
- Bhushan, a et al., 2001. Fgf10 is essential for maintaining the proliferative capacity of epithelial progenitor cells during early pancreatic organogenesis. *Development*, 128(24), pp.5109–5117.
- Borthwick, D.W. et al., 1999. Murine submucosal glands are clonally derived and show a cystic fibrosis gene-dependent distribution pattern. *American Journal of Respiratory Cell and Molecular Biology*, 20(6), pp.1181–9.
- Bradley, A. et al., 2012. The mammalian gene function resource: The International Knockout Mouse Consortium. *Mammalian Genome*, 23(9–10), pp.580–586.
- Buisine, M.P. et al., 1999. Developmental mucin gene expression in the human respiratory tract. *American journal of respiratory cell and molecular biology*, 20(2), pp.209–218.
- Callea, M. et al., 2013. Ear nose throat manifestations in hypoidrotic ectodermal dysplasia. *International Journal of Pediatric Otorhinolaryngology*, 77(11), pp.1801–4.
- Chatzeli, L., Gaete, M. & Tucker, A.S., 2017. Fgf10 and Sox9 are essential for the establishment of distal progenitor cells during mouse salivary gland development. *Development*, 144(12), pp.2294–2305.
- Cho, H.-J., Joo, N.S. & Wine, J.J., 2011. Defective fluid secretion from submucosal glands of nasal turbinates from CFTR<sup>-/-</sup> and CFTR ( $\Delta$ F508/ $\Delta$ F508) pigs. N. Vij, ed. *PloS one*, 6(8), p.e24424.
- Danielian, P.S. et al., 1998. Modification of gene activity in mouse embryos in utero by a tamoxifen-inducible form of Cre recombinase. *Current biology : CB*, 8(24), pp.1323–1326.
- Entesarian, M. et al., 2007. FGF10 missense mutations in aplasia of lacrimal and salivary glands (ALSG). *European Journal of Human Genetics*, 15(3), pp.379–82.



- Finkbeiner, W.E., 1999. Physiology and pathology of tracheobronchial glands. *Respiration Physiology*, 118(2–3), pp.77–83.
- Hajihosseini, M.K. 2008. Fibroblast growth factor signalling in cranial suture development and pathogenesis. *Frontiers in Oral Biology*, 12, pp.160-177
- Hannezo, E. et al., 2017. A Unifying Theory of Branching Morphogenesis. *Cell*, 171(1), pp.242–255.e27.
- Hayashi, S. & McMahon, A.J. 2000. Efficient recombination in diverse tissues by a tamoxifen-inducible form of cre: a tool for temporally regulated gene activation/inactivation in the mouse. *Developmental Biology*, 244; pp. 305-318
- Hoegger, M.J. et al., 2014. Impaired mucus detachment disrupts mucociliary transport in a piglet model of cystic fibrosis. *Science*, 345(6198), pp.818–22.
- Ianowski, J.P. et al., 2007. Mucus secretion by single tracheal submucosal glands from normal and cystic fibrosis transmembrane conductance regulator knockout mice. *The Journal of Physiology*, 580(Pt 1), pp.301–14.
- Jaskoll, T. et al., 2005. FGF10/FGFR2b signaling plays essential roles during in vivo embryonic submandibular salivary gland morphogenesis. *BMC Developmental Biology*, 5, p.11.
- Jeong, J.H. et al., 2015. Secretion rates of human nasal submucosal glands from patients with chronic rhinosinusitis or cystic fibrosis. *American journal of rhinology & allergy*, 29(5), pp.334–338.
- Joo, N.S. et al., 2001. Optical method for quantifying rates of mucus secretion from single submucosal glands. *American Journal of Physiology. Lung Cellular and Molecular Physiology*, 281(2), pp.L458-68.
- Joo, N.S. et al., 2010. Hyposecretion of fluid from tracheal submucosal glands of CFTR-deficient pigs. *The Journal of clinical investigation*, 120(9), pp.3161–3166.
- Kelly, R.G. et al., 2001. The arterial pole of the mouse heart forms from Fgf10-expressing cells in pharyngeal mesoderm. *Developmental Cell*. 1, pp.435–440.
- Keswani, S.G. et al., 2011. Submucosal gland development in the human fetal trachea xenograft model: implications for fetal gene therapy. *Journal of Pediatric Surgery*, 46(1), pp.33–8.
- Klockars, M. & Reitamo, S., 1975. Tissue Distribution of Lysozyme in Man. *Journal of Histochemistry & Cytochemistry*, 23(12), pp.932–940.
- Lizen, B. et al., 2015. Perinatal induction of Cre recombination with tamoxifen. *Transgenic Research*, 24, pp1065-1077.

- Lynch, T.J. et al., 2018. Submucosal Gland Myoepithelial Cells Are Reserve Stem Cells That Can Regenerate Mouse Tracheal Epithelium. *Cell Stem Cell*, 22(5), pp.653–667.
- Mailleux, A.A. et al., 2002. Role of FGF10/FGFR2b signaling during mammary gland development in the mouse embryo. *Development*, 129, pp.53–60.
- Makarenkova, H.P. et al., 2000. FGF10 is an inducer and PAX6 a competence factor for lacrimal gland development. *Development*, 127, pp.2563–2572.
- Masson, P.L. et al., 1966. Immunohistochemical localization and bacteriostatic properties of an iron-binding protein from bronchial mucus. *Thorax*, 21(6), pp.538–44.
- May, A. & Tucker, A., 2015. Understanding the development of the respiratory glands. *Developmental Dynamics*, 244(4), pp.525–539.
- May, A.J. et al., 2016. FGF and EDA pathways control initiation and branching of distinct subsets of developing nasal glands. *Developmental Biology*, 419(2), pp.348–356.
- May, A.J. et al., 2015. Salivary Gland Dysplasia in Fgf10 Heterozygous Mice: A New Mouse Model of Xerostomia. *Current Molecular Medicine*, pp.1–9.
- Milunsky, J.M. et al., 2006. LADD syndrome is caused by FGF10 mutations. *Clin Genet*, 69(4), pp.349–354.
- Min, H. et al., 1998. Fgf-10 is required for both limb and lung development and exhibits striking functional similarity to Drosophila branchless. *Genes & Development*, 12(20), pp.3156–3161.
- De Moerloose, L. et al., 2000. An important role for the IIIb isoform of fibroblast growth factor receptor 2 (FGFR2) in mesenchymal-epithelial signalling during mouse organogenesis. *Development*, 127(3), pp.483–92.
- Oppenheimer, E. & Esterly, J., 1975. Pathology of cystic fibrosis: review of the literature and comparison with 146 autopsied cases. In H. Rosenberg & R. Bolande, eds. *Perspectives in Pediatric Pathology*. Chicago, USA: Yearbook Medical Publishers, pp. 241–278.
- Ornitz, D. & Itoh, N., 2001. Fibroblast growth factors. *Genome Biology*, 2(3), pp.1–12.
- Ramasamy, S.K. et al., 2007. Fgf10 dosage is critical for the amplification of epithelial cell progenitors and for the formation of multiple mesenchymal lineages during lung development. *Developmental Biology*, 307(2), pp.237–247.
- Rawlins, E. et al., 2009. The Role of Scgb1a1+ Clara Cells in the Long-Term Maintenance and Repair of Lung Airway, but Not Alveolar, Epithelium. *Cell Stem Cell*, 4(6), pp.525–534.

- Rawlins, E.L. et al., 2007. Lung development and repair: contribution of the ciliated lineage. *Proceedings of the National Academy of Sciences of the United States of America*, 104(2), pp.410–7.
- Rawlins, E.L. & Hogan, B.L.M., 2005. Intercellular growth factor signaling and the development of mouse tracheal submucosal glands. *Developmental Dynamics*, 233(4), pp.1378–85.
- Reid, L., 1960. Measurement of the bronchial mucous gland layer: a diagnostic yardstick in chronic bronchitis. *Thorax*, 15, pp.132–41.
- Rock, J.R. et al., 2009. Basal cells as stem cells of the mouse trachea and human airway epithelium. *Proceedings of the National Academy of Sciences of the United States of America*, 106(31), pp.12771–5.
- Rogers, D.F., 2004. Airway mucus hypersecretion in asthma: an undervalued pathology? *Current Opinion in Pharmacology*, 4(3), pp.241–50.
- Rogers, D.F., 2008. Airway Mucus Hypersecretion in Asthma and COPD: Not the Same? In P. Barnes et al., eds. *Asthma and COPD. Basic Mechanisms and Clinical Management*. Academic Press Inc., pp. 211–223.
- Roy, M.G. et al. 2014. Muc5b is required for airway defense. *Nature*. 505, pp412-416.
- Sala, F.G. et al., 2011. FGF10 controls the patterning of the tracheal cartilage rings via Shh. *Development*, 138, pp.273–282.
- Salinas, D. et al., 2005. Submucosal gland dysfunction as a primary defect in cystic fibrosis. *FASEB journal : official publication of the Federation of American Societies for Experimental Biology*, 19(3), pp.431–433.
- Sekine, K. et al., 1999. Fgf10 is essential for limb and lung formation. *Nature Genetics*, 21(1), pp.138–141.
- Shams, I. et al., 2007. Lacrimo-auriculo-dento-digital syndrome is caused by reduced activity of the fibroblast growth factor 10 (FGF10)-FGF receptor 2 signaling pathway. *Mol Cell Biol*, 27(19), pp.6903–6912.
- Skarnes, W.C. et al., 2011. A conditional knockout resource for the genome-wide study of mouse gene function. *Nature*, 474(7351), pp.337–344.
- Steinberg Z. et al., 2005. FGFR2b signaling regulates ex vivo submandibular gland epithelial cell proliferation and branching morphogenesis. *Development* 132, pp.1223-1234.
- Sturgess, J. & Imrie, J., 1982. Quantitative evaluation of the development of tracheal submucosal glands in infants with cystic fibrosis and control infants. *The American Journal of*

1009  
1010  
1011 *Pathology*, 106(3), pp.303–11.

1012  
1013 Song, Y. et al., 2001. Role of aquaporin water channels in airway fluid transport, humidification ,  
1014 and surface liquid hydration. *J Gen Physiol* 17, pp 573-582.

1015  
1016 Teshima, T.H.N., Lourenço, S.V. & Tucker, A.S., 2016. Multiple Cranial Organ Defects after  
1017 Conditionally Knocking Out Fgf10 in the Neural Crest. *Frontiers in physiology*, 7, p.488.

1018  
1019 Thurlbeck, W., Benjamin, B. & Reid, L., 1961. Development and distribution of the mucous  
1020 glands in the foetal human trachea. *British Journal of Diseases of the Chest*, 55, pp.54–64.

1021  
1022 Wells, K.L. et al., 2013. Dynamic relationship of the epithelium and mesenchyme during  
1023 salivary gland initiation: the role of Fgf10. *Biology open*, 2(10), pp.981–989.

1024  
1025 Xie, W. et al., 2014. Sox2 modulates Lef-1 expression during airway submucosal gland  
1026 development. *AJP: Lung Cellular and Molecular Physiology*, 306(7), pp.L645–L660.

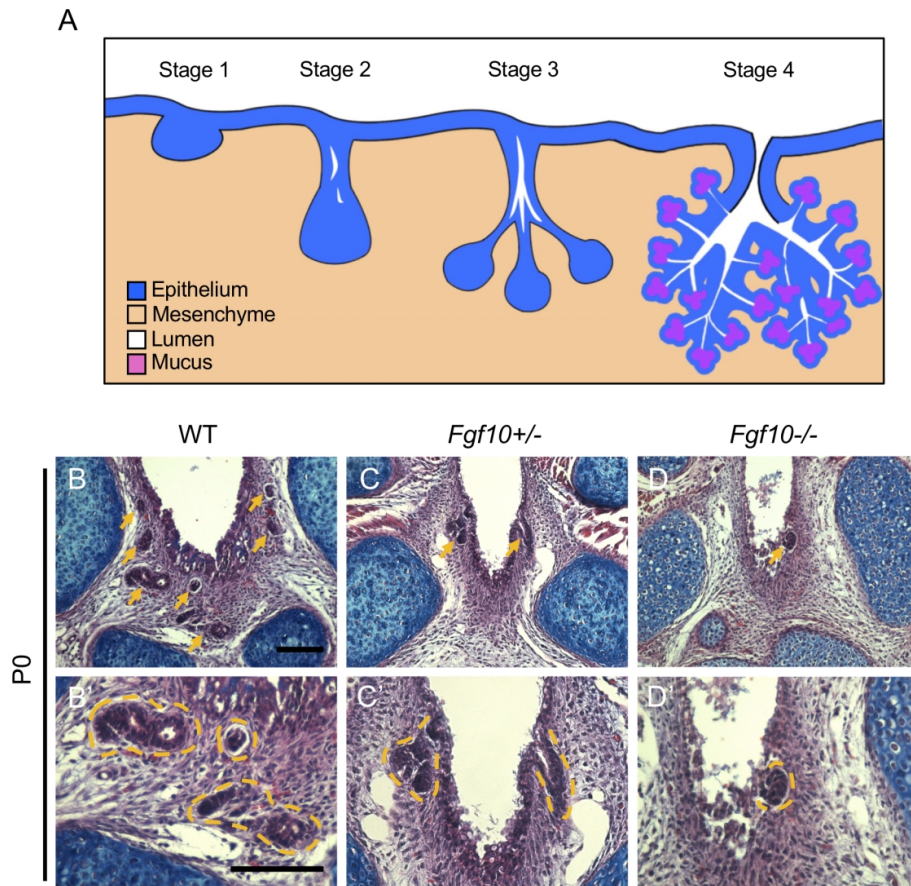


**Figure 1. *Fgf10* is essential for successful tracheal gland branching morphogenesis.**

**(A)** Schematic representation of the four stages of tracheal gland branching morphogenesis. Stage 1: Tracheal SMG buds first invaginate from the respiratory epithelium into the underlying mesenchyme. Stage 2: Elongation of the bud occurs, and cavitation begins lumen formation. Stage 3: Epithelial stalk undergoes clefting and branching and lumen formation continues. Stage 4: Continual branching and cellular differentiation occurs indicated by mucus production by acinar cells. (B-D) Frontal trichrome stained images of the anterior trachea at postnatal stage (P) 0. (B'-D') High power images of B-D. (B, B') WT SMGs reached lumen formation and branching stages in the ventral trachea at P0. (C, C') *Fgf10*<sup>+/-</sup> SMGs form lumens, however branching of the glands was reduced. (D, D') Gland buds were found in *Fgf10*<sup>-/-</sup> mice however they had not elongated from the respiratory epithelium. Scale bar in B, B' = 100μm, same scale in other images. Arrows indicate SMGs, orange outline SMGs in higher magnification images. Cartilages stain blue with alcian blue.

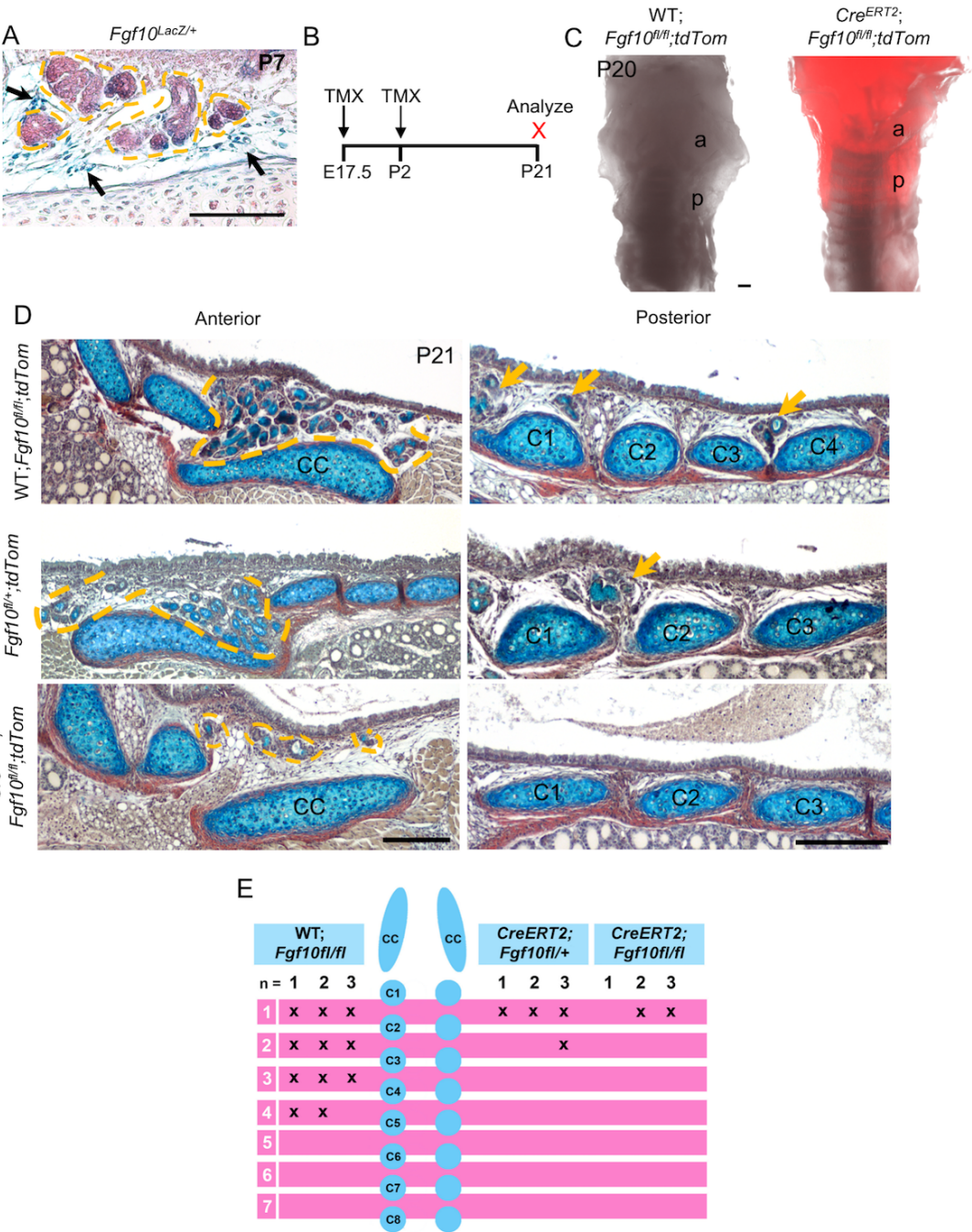


**Figure 2. Tracheal SMG morphogenesis is inhibited with conditional ablation of *Fgf10* during postnatal SMG development.**

**(A)** *Fgf10*<sup>LacZ/+</sup> trachea at postnatal day (P) 7 stained with X-gal (blue – arrows) to show *Fgf10* expression surrounding SMGs. **(B)** Time-course of tamoxifen (TMX) administration of wildtype (WT) and *Cre*<sup>ERT2</sup>;*Fgf10*<sup>fl/fl</sup>;*tdTom* mice. TMX was given to pregnant females at embryonic day (E)17.5 and individual pups on P2. Trachea were analyzed on P21. **(C)** Confirmation of inducible *Cre* recombination in the anterior (a) and posterior (p) trachea by the expression of R26tdTomato (red). **(D)** A significant loss in anterior SMG branching is evident in P21 *Fgf10* conditional knock-out mice adjacent to the cricoid cartilage (CC), with a reduction in SMG branch expansion into the mesenchyme compared to WT. Heterozygous mice showed a slight reduction in anterior SMG branching. **(D, E)** Posterior SMGs are present between the cartilage rings (C1-C4) in WT animals at P21, however are reduced in heterozygous and homozygous *Fgf10* mutant mice. Scale bar in A = 100µm, C & D = 200µm. Orange outline indicates anterior SMGs. Arrows indicate posterior SMGs.



1233  
1234  
1235  
1236  
1237  
1238  
1239  
1240  
1241  
1242  
1243  
1244  
1245  
1246  
1247  
1248  
1249  
1250  
1251  
1252  
1253  
1254  
1255  
1256  
1257  
1258  
1259  
1260  
1261  
1262  
1263  
1264  
1265  
1266  
1267  
1268  
1269  
1270  
1271  
1272  
1273  
1274  
1275  
1276  
1277  
1278  
1279  
1280  
1281  
1282  
1283  
1284  
1285  
1286  
1287  
1288

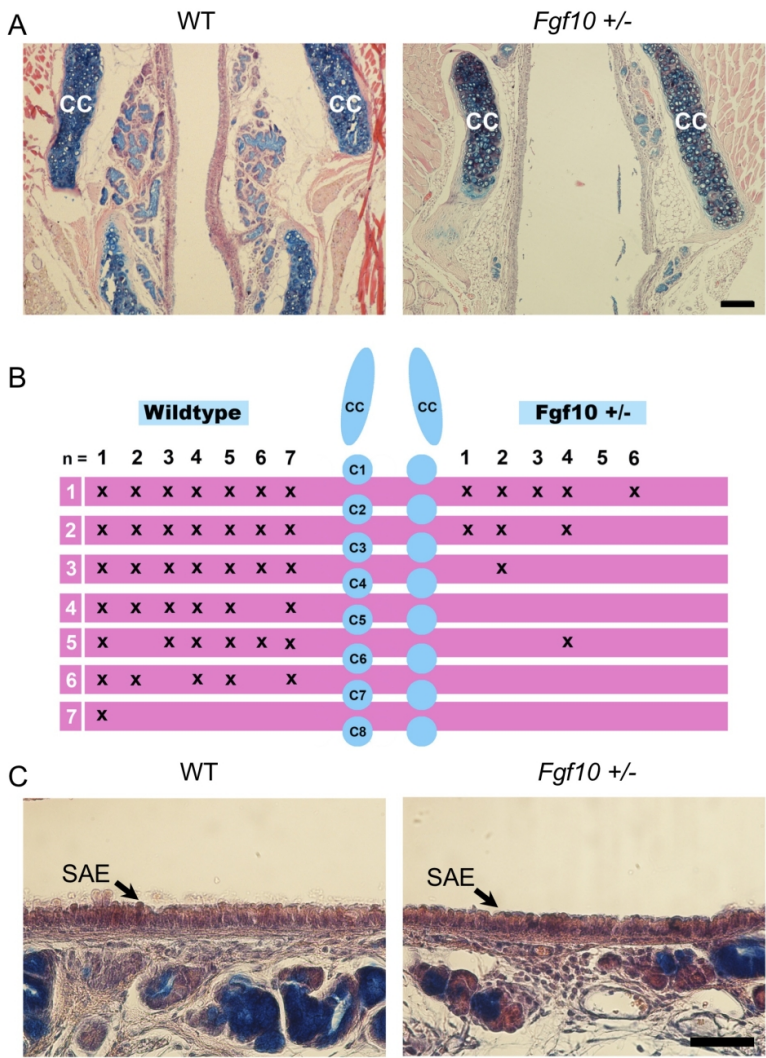


**Figure 3. *Fgf10* +/- tracheal SMG phenotype is not recovered in adult animals.**

**(A,C)** Frontal sections through adult tracheas stained with trichrome. **(A)** WT adults show extensively branched anterior SMGs adjacent to the cricoid cartilage (CC) while *Fgf10* +/- littermates show a significant reduction in glands in a similar plane. Scale bar = 100µm. **(B)** Posterior extension of the SMGs is noticeably reduced in *Fgf10* +/- animals compared to their WT littermates. N numbers represent each specimen analysed while pink bars represent mesenchymal space where SMGs are found between each cartilage ring (C1-C8). X indicates presence of SMG. **(C)** No obvious differences were observed in the tracheal epithelium of adult WT and *Fgf10* +/- littermates at 6-10 weeks. Scale bar in A, C = 50µm.



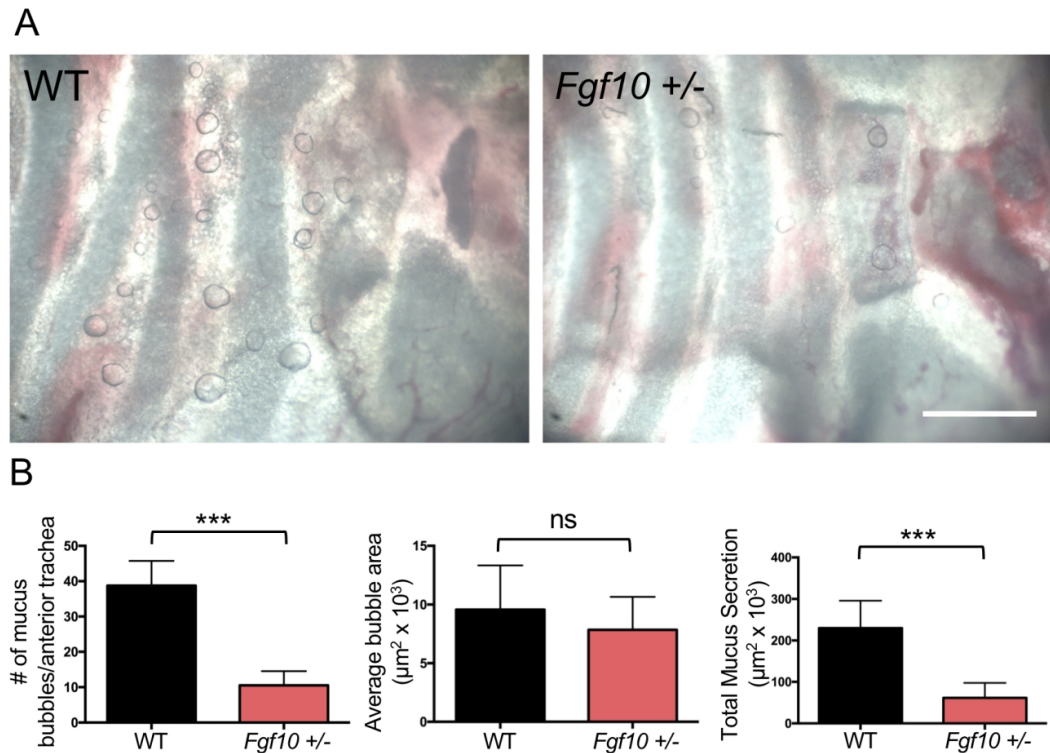
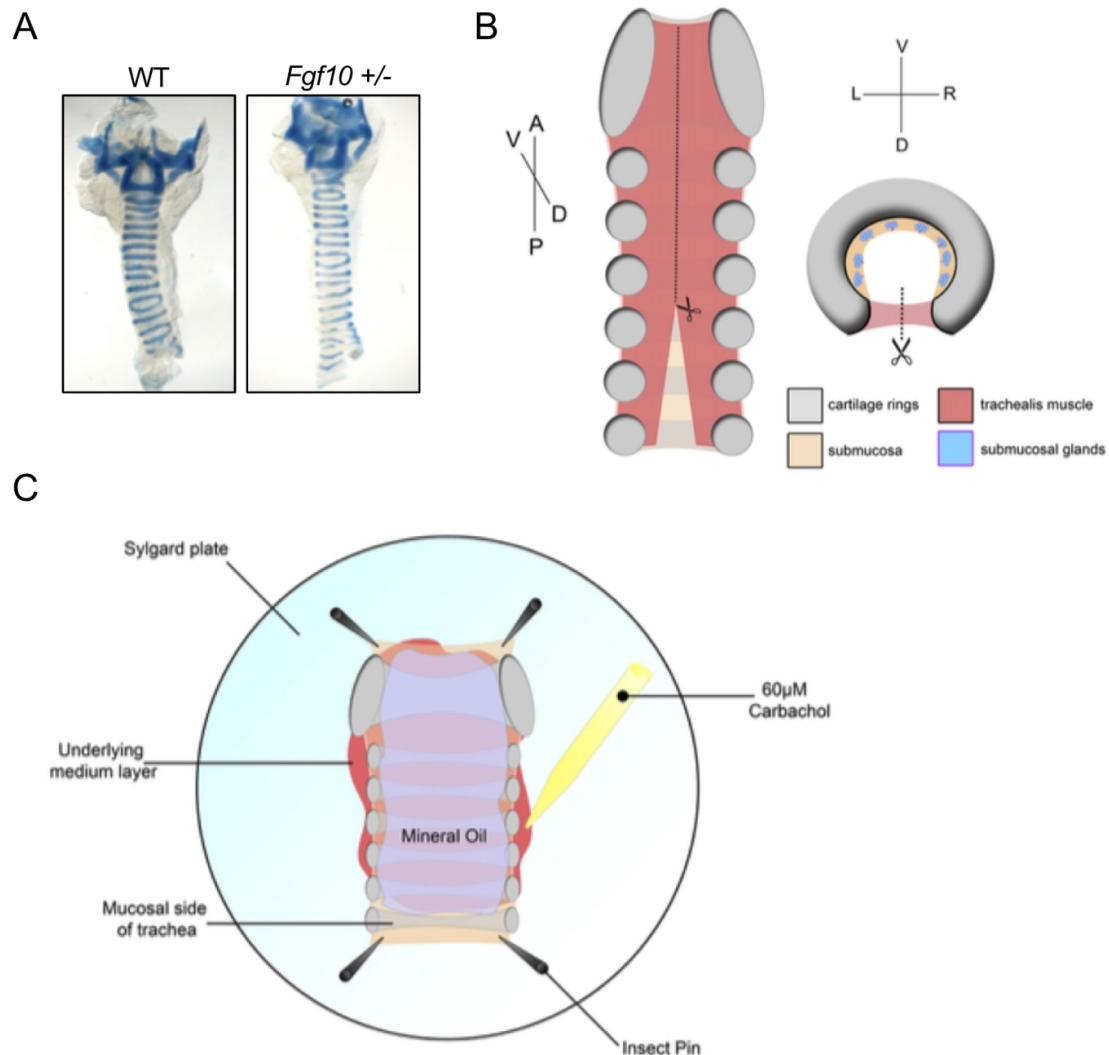


**Figure 4. *Fgf10* +/- adult mice have fewer tracheal SMGs and an overall reduction in mucus secretion.**

**(A)** Visualisation of functional gland openings in WT (n=4) and *Fgf10* +/- (n=6) anterior tracheal tissue by mucus bubble production. A decrease in the number of mucus bubbles was observed in *Fgf10* +/- mice. Scale bar = 500 $\mu\text{m}$ . **(B)** Graphical representation of mucus bubble count, showing a significant reduction in *Fgf10* +/- animals compared to their WT littermates. Average bubble area was similar between the two groups however overall mucus secretion into the airway lumen was significantly reduced in *Fgf10* +/- animals. \*\*\* =  $p < 0.001$ . Data in B are mean  $\pm$  s.d.



**Supplementary Figure 1.**

**(A)** WT and *Fgf10* +/- show no differences in tracheal cartilage ring patterning at E18.5. **(B)** Schematic representation of dissection protocol carried out on adult tracheal tissue in preparation for mucus production analysis. Axis labels: anterior (A); posterior (P); ventral (V), dorsal (D); left (L); right (R). **(C)** For mucus secretion analysis, tracheal tissue was flattened out and pinned down onto a sylgard plate, exposing the mucosal side. DMEM F/12 medium was added underneath the tissue, while mineral oil was added on top of the mucosal side and gland openings. After 10 minutes of incubation, carbachol was added to the medium bath. Mucus bubble production was observed and recorded for 10 minutes.